© 2003 The Chemical Society of Japan

Molecular Modeling of the Solvent Structuring of DMSO around Cellulose Triacetate

Isseki Yu, Kazuyoshi Ueda,* and Haruo Nakayama

Department of Material Science, Faculty of Engineering, Yokohama National University, 79-5 Tokiwadai, Hodogaya-ku, Yokohama 240-8501

(Received August 16, 2002)

Molecular dynamics simulations of cellulose triacetate (CTA) were performed with explicit DMSO molecules in order to investigate the solvent structuring of DMSO around the CTA polymer. A hexamer unit of CTA was used as a model instead of polymer CTA. The molecular dynamics trajectory was started from a minimum conformation, which was found from an analysis of the adiabatic potential-energy surface obtained for glycosidic dihedral angles of ϕ and ψ. It showed that most of the time the trajectory stayed in their initial conformation in DMSO solvent. A distance analysis between the acetyl methyl residues of CTA showed that they are in good accordance with the NMR-NOESY data obtained by Tezuka.[1] In order to elucidate the solvation structure of DMSO around the solute molecules, the site-specified radial distribution function, the orientation and the time courses of the DMSO movement were analyzed precisely. The results showed that some DMSO molecules strongly interact with CTA at specific sites, such as acetyl methyl residues and H1 ring protons. Moreover, it was found that those DMSO molecules frequently interact to CTA, not with one site, but with two or more sites simultaneously. These DMSO molecules would play an important role in the conformation of CTA in this solvent.

Cellulose is a polysaccharide which consists of 1–4 linked β-D-glucopyranoses. It is the most popular and the most abundant material in the world, and has a close relation to human life as paper, textile, and housing materials. From many years ago, much effort has been continued to improve the properties of cellulose in order to add new functions to it.[2] One such effort is to develop cellulose derivatives. Cellulose triacetate (CTA) is produced by acetylating three hydroxy residues at the 2, 3, and 6 positions on cellulose, and has been used as photograph film and cigarette filter for many years.[3] Although it is an old material, it again recently begun to attract attention through such applications as medical polymers and functional materials.[4–6] However, its use in these fields needs more understanding concerning the basic properties of the solution, such as the solubility, film properties, and micro-structure in solution in order to improve and control the product quality. Although many studies have been performed on the macroscopic properties of CTA, that from a microscopic aspect, such as the conformation, dynamics, and molecular details concerning the solvation of CTA in solution, has still quite few in number.[1,7,8]

In the solid state, the conformation of CTA has already well investigated, and X-ray and electron diffraction analyses have indicated that there are two morphologies of CTA I and II, which correspond to cellulose I and II, respectively.[9–13] Although the main-chain conformations are a 2/1 helix in both cases, they are different in the chain orientation. The chains align in parallel in the CTA I structure, while they align antiparallel in CTA II. On the other hand, the conformation of CTA in solution is still ambiguous. Buchanan et al.[8] measured the NMR signals of CTA in solvents and observed an unusual response to the temperature and concentration. From an analysis of NOESY signals, they proposed that CTA takes a 5/4 helix in chloroform. Tezuka[1] measured the NOESY-NMR spectra of CTA in DMSO and observed that there were two strong NOE signals, one between the 2 and 6 positions and the other is between the 3 and 6 positions of acetyl residues. On the other hand, in a chloroform solution, he observed only one NOE signal between the 3 and 6 positions of acetyl residues. This indicated that CTA has a possibility to exist in different conformations between the solvents.

The molecular dynamics simulation is one of the most powerful methods to investigate the molecular conformation when used in combination with the NMR information. This is well established, especially in the field of protein analysis.[14] However, it seems that until now, no investigation of the conformation of CTA in solution using a molecular dynamics simulation has been performed. In an attempt to obtain information about the relationship between the solvent and the conformation of CTA, we planned to make a series of studies by using molecular dynamics simulations. In this work, a molecular dynamics simulation was performed in DMSO solvent using hexamer CTA as a model of CTA polymer. From the time courses of the simulation, the solvated structure of DMSO molecules to CTA, the conformation of CTA, and their dynamics were investigated precisely. The results indicated that the DMSO molecules take specific solvated coordinations to acetyl residues of CTA. The specific orientation of DMSO solvent would seem to be an important factor on the acetyl residue orientation and the main chain conformation of CTA in this solvent.

In an application field, like optical use, information concerning the microscopic conformation directly relates to the

control of such functions as the refractive indices. The molecular level information will be expected to become more important in the future for the development of new materials with controlled three-dimensional structures and with designed nano-structures.

Methods

Nomenclature. The structure and the nomenclature of the CTA hexamer used in this paper are shown in Fig. 1. The monomers are numbered sequentially from the non-reducing end. If needed, the atom names are expressed along with their residue number, which was attached before each atom name. The reducing and non-reducing ends are hydroxy groups in our model. The dihedral angles (ϕ, ψ) of the glycosidic bonds are defined as ϕ: *n*C2–*n*C1–*n*O1–(n + 1)C4 and ψ: *n*C1–*n*O1–(n + 1)C4–(n + 1)C3, n = 1–5, respectively. The dihedral angles of acetyl residue are defined as χ21: *n*H2–*n*C2–*n*O2–*n*CAc2, χ22: *n*C2–*n*O2–*n*CAc2–OAc2, χ31: *n*H3–*n*C3–*n*O3–*n*CAc3, χ32: *n*C3–*n*O3–*n*CAc3–OAc3, χ61: *n*O5–*n*C5–*n*C6–*n*O6, χ62: *n*C5–*n*C6–*n*O6–*n*CAc6, χ63: *n*C6–*n*O6–*n*CAc6–*n*OAc6, respectively.

Parameterization. Molecular mechanics and molecular dynamics calculations were performed using the CHARMM25 program.[15] Ha's force field parameter set for sugar[16] was used in this calculation. Since the parameters for the acetyl residue are not included in Ha's set, those parameters were derived in this study by fitting CHARMM force field functions to the energy curves obtained by ab initio SCF calculations by using a nonlinear least-squares method. The formula of the force field functions for CHARMM25 are shown in Eq.1 of a reference.[15] Because the force constants of the bonds and angles were generally insensitive to the conformation at ambient temperature, only the dihedral parameters were determined in this work, and other parameters for bonds and angles were taken from similar atom types in CHARMM25. Isopropyl acetate was used as a model molecule to make the force field parameter for the acetyl residue. In order to obtain the parameters of the dihedral angles of H–C–O–CAc and CA–C–O–CAc, the dihedral angle of H–C–O–CAc for isopropyl acetate was rotated from 0° at the *cis* position to 180° with a 30° interval increment. At each position, the potential energy of this molecule was obtained by ab initio optimization. In the above calculation, all of the dihedral angles, except for the dihedrals corresponding to the rotation around the C–O bond, were fixed at their optimized positions. Ab initio optimizations were performed using Gaussian94 with an RHF 6-31G* basis set.[17]

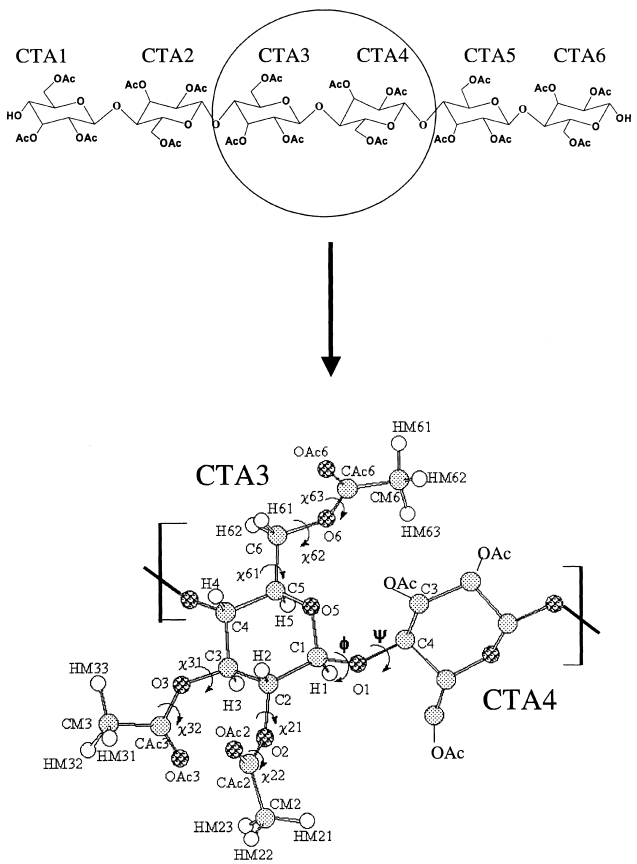

Fig. 1. Schematic structure of cellulose triacetate hexamer and the nomenclature of its monomer unit. The definitions of the dihedral angles are also shown in the figure.

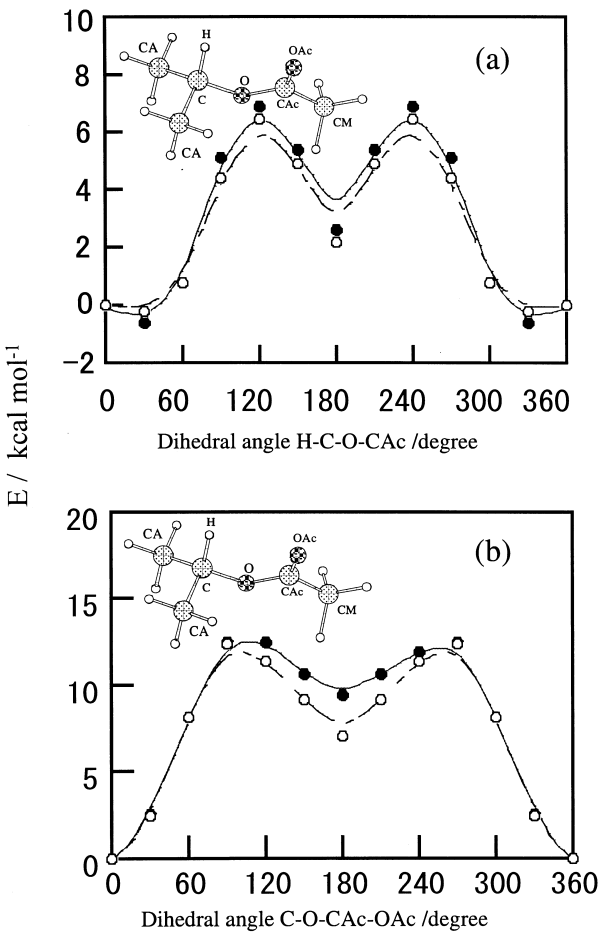

Fig. 2. Comparison of the CHARMM (○) and ab initio (●) potential energy curves for the rotation around C–O bond (a) and O–CAc bond (b) for the isopropyl acetate. The abscissa were plotted by using the dihedral angles of H–C–O–CAc (a) and C–O–CAc–OAc (b), respectively.

The calculated ab initio potential-energy curve and the fitted one with the obtained CHARMM function are shown in Fig. 2 (a). In this case, as a result, it was found that no dihedral forces were needed to reproduce the energy profile around the rotation of the C–O bond, which was obtained by an ab initio calculation. In a similar manner, the parameters of the dihedral angles of C–O–CAc–OAc and C–O–CAc–CM were determined, the results are shown in Fig. 2 (b) in terms of dihedral rotation around the O–CAc bond. Although there are some discrepancies in the high-energy regions, it can be seen that the fitted CHARMM function well reproduced the potential-energy profile of the ab initio calculation, especially in the low-energy region, where the energy profile is important at ambient temperature. The obtained parameters are listed in Table 1.

The partial atomic charges of the acetyl residue were calculated by the following procedure using the optimized monomer unit of CTA. There are various conformers according to the rotation of three acetyl residues on the monomer unit of CTA. Therefore, the initial structures of the monomer unit were constructed by considering all of the combination of dihedral values of 60°, 180°, 300° for every χ21, χ31, χ61, and χ62 dihedrals. Each initial conformation of the monomer unit was first optimized by MOPAC PM3,[18] and the lowest energy conformation was obtained. This structure was further optimized by using the Gaussian94 program with the 6-31G* base set, and the fully optimized lowest energy conformation and partial charges for this monomer molecule were obtained. The Merz-Singh-Kollman method was used to calculate the partial electric charge.[19,20] Based on the partial charges obtained above, the atomic charges for the glucose ring atoms were redistributed to give a priority to the Ha's existing value. On the other hand, the partial atomic charges for the acetyl residue were determined with priority given to the values of an ab initio calculation of the monomer unit of CTA. The resulting partial charges are given in Table 2.

The dihedral angles of the obtained energy minimum conformation of the monomer unit are listed in Table 3. The dihedral angles of χ21 and χ31 were twisted by about 30° from the *cis* position, and χ61 was 68°. As the staggered conformation of the hydroxymethyl group, χ61, is defined by using two dihedral angles of O5–C5–C6–O6 and C4–C5–C6–O6 as *gauche-gauche* (*gg*) *gauche-trans* (*gt*) and *trans-gauche* (*tg*), the above values of χ61 correspond to the *gt*-type conformation. Other dihedral angles of χ22, χ32, and χ63 showed nearly perfect *cis* positions and χ62 showed a *trans* position, respectively. Although the global minimum conformation of χ61 is the *gt* conformation, the energy difference of the other staggered conformations of *gg* and *tg* were examined by rotating only the χ61 dihedral from the global minimum *gt* conformation. The results showed that the energies of both the *gg* and *tg* conformations are within 1 kcal/mol from the global minimum. This indicates that all of the staggered conformations have almost the same energies in the monomer unit.

Table 1. Force Field Parameters for Acetyl Residue

Dihedral type	K_θ/kcal mol^{-1}	n	Phase
C–O–CAc–OAc	0.38	1	180
C–O–CAc–OAc	2.27	2	180
C–O–CAc–CM	2.27	2	180
H–C–O–CAc	0.0	3	0
CA–C–O–CAc	0.0	3	0

Table 2. Partial Atomic Charges of CTA Used in Charmm Calculation. The Values Obtained from Ab Initio Calculation Were Also Shown as a Comparison

Atom	Charmm	Gaussian 6-31 g*
H2	0.10	0.13
C2	0.15	0.13
O2	−0.56	−0.57
CAc2	1.00	1.02
OAc2	−0.60	−0.62
CM2	−0.60	−0.59
HM21	0.17	0.19
HM22	0.17	0.15
HM23	0.17	0.17
H3	0.10	0.07
C3	0.15	0.32
O3	−0.56	−0.56
CAc3	1.00	0.93
OAc3	−0.60	−0.65
CM3	−0.60	−0.63
HM31	0.17	0.17
HM32	0.17	0.19
HM33	0.17	0.16
C6	0.15	0.32
O6	−0.56	−0.57
CAc6	1.00	1.02
OAc6	−0.60	−0.65
CM6	−0.60	−0.61
HM61	0.17	0.17
HM62	0.17	0.18
HM63	0.17	0.16
H61	0.05	0.06
H62	0.05	0.05
H5	0.10	0.02
C5	0.30	0.40
C1	0.40	0.54
H1	0.10	−0.01
C4	0.15	−0.02
O4	−0.65	−0.70
H4	0.10	0.08
O5	−0.60	−0.58

As far as we know, all of the available parameters for DMSO molecules in the literature treat the methyl group as a united atom, as summarized by Skaf.[21] However, our parameter of CTA is an all-atom type force field. This parameter takes into account the polar property of the methyl group of CTA because of their partial charges. Therefore, the choice of the model for DMSO should also take into account the polar effect of the methyl groups in order to balance the parameters between CTA and DMSO. In this study, we chose the force-field parameter for DMSO developed by Liu et al,[22] because this was designed to reproduce the polar effect of methyl groups within a united atom model by adjusting the length of the C–S bond. This model treats DMSO as a rigid molecule with S, O,

Table 3. Summary of the Dihedral Angles of the Monomer Unit for CTA Obtained by Ab Initio Calculation and the Characteristic Features of the Local Energy Minimum Structures Obtained from Adiabatic Potential Energy Surface for Dimer Unit of Cellulose Triacetate

		Potential minimum wells				
	Dihedrals	Monomer	A	B	C	D
ϕ/degrees			182	124	258	182
ψ/degrees			121	77	123	310
Energy/kcal mol^{-1}			0.0	1.45	3.12	0.55
	χ21	25	3	25	16	5
Dihedral	χ22	3	1	2	5	1
angles of	χ31	30	26	24	20	19
acetyl / degrees	χ32	−4	1	0	−1	−1
residue	χ61	68 (*gt*)	66 (*gt*)	72 (*gt*)	−61 (*gg*)	59 (*gt*)
at CTA1	χ62	177	−111	−125	90	−113
	χ63	0	0	0	2	2
	χ21		2	8	23	17
Dihedral	χ22		−1	2	3	1
angles of	χ31		−15	21	180	4
acetyl / degrees	χ32		2	4	3	−1
residue	χ61		145 (*tg*)	153 (*tg*)	153 (*tg*)	166 (*tg*)
at CTA2	χ62		133	165	129	119
	χ63		−4	2	0	3

and the two CH_3 (united atoms), which are named SDM, ODM , CD1, and CD2 in this study, respectively.

Calculation Procedures. An adiabatic potential-energy map for the glycosidic dihedral angles of ϕ and ψ was calculated using the dimer unit of CTA according to the same method described in previous papers.[23–25] This method is briefly described as follows. The dihedral angles of ϕ and ψ were separately rotated with an increment of 20°, and an energy minimization was performed at each set of ϕ and ψ. In the above minimization, the combination of all staggered conformations of acetyl residues were taken into account to search for the lowest energy conformation at each ϕ and ψ. In the calculation of map, a dielectric constant of 4 was used to approximate the electrostatic screening of the surrounding media in a conventional manner.[26]

A molecular dynamics simulation of hexamer CTA in DMSO was performed as follows. The CTA hexamer was put at the center of a 55 Å × 55 Å × 80 Å box filled with pre-equilibrated DMSO molecules, and then these DMSO molecules which overlapped with the CTA hexamer were eliminated. To relax the solvent molecules around the solute CTA, several steps of energy minimization were performed with the conjugate gradient minimization method. The resulted conformation was used as a starting structure of the simulation. Periodic boundary conditions were assigned to the box. Since an accurate solution density of CTA hexamer was not found in the literature, it was adjusted to the pure DMSO solvent of 1.095 g/cm^3. The final box size was 55 Å × 55 Å × 80 Å, which included 2020 DMSO molecules around the CTA hexamer. The trajectories were integrated using the Verlet method with a time step of 1 fs by a NVE ensemble. The electrostatic interaction was calculated using the Ewald method.[27] After the system was equilibrated at 300 K for the first 20 ps by restraining all glycosidic angles of ϕ and ψ, a free simulation of 1000 ps was performed for an analysis.

Results and Discussion

Conformational Energy Map of CTA Dimer. The conformation of CTA is mainly determined by the glycosidic dihedral angles between adjoining glucose rings. Therefore, we first prepared an adiabatic potential energy map for the rotation of the ϕ and ψ dihedral angles using the dimer unit of CTA. Figure 3 shows the obtained potential-energy map for this dimer. This map indicates the existence of four potential-energy minima in the map from the A well to the D well. The dihedral values and the potential energy at each minimum point are given in Table 3 along with its acetyl residues conformation.

The small filled circles (X1–X5) on the map summarized the previously reported values of ϕ and ψ obtained from X-ray diffraction experiments of crystalline CTA by several researchers. The point at X1 was the value of β-D-acetyl cellobiose[28] and point X2 was the value between the reducing and middle residues of β-Cellotriose undecaacetate,[29] respectively. Both of these values locate close to the A well. On the other hand, the other dihedral of β-Cellotriose undecaacetate between non-reducing and middle residues located on the saddle point between the A and B wells, as shown by X3. Furthermore, the values obtained for polymer CTA II (X4)[13] and CTA I (X5)[9] are also located in a similar saddle area. Polymer effects and/or inter-chain interactions in the crystalline state may shift the conformation. A similar behavior was observed for the case of cellulose, whose crystal structure is located on the saddle point between the minima in the potential map calculated by Hardy and Sarko.[30]

Table 3 shows that the acetyl residue conformations at χ61 differ from one another in the wells and in residues. As we al-

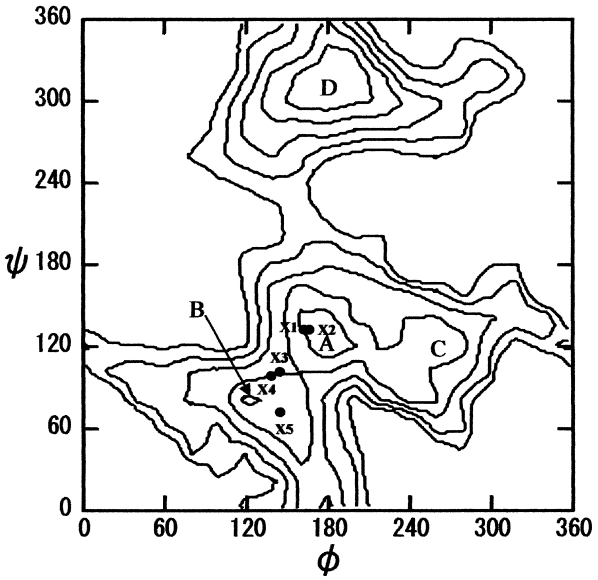

Fig. 3. The (ϕ, ψ) adiabatic potential energy surface for cellulose triacetate dimer. Contours are in 2 kcal/mol intervals. The local minima are indicated by capital letters from A to D. The experimentally obtained values of the dihedral angles for the crystal structures are indicated by (●) from X1 to X5. Those are X1 (ϕ = 165°, ψ = 134°) for β-D-acetyl cellobiose, X2 (ϕ = 169°, ψ = 134°) for β-Cellotriose undecaacetate between the reducing and middle residues, X3 (ϕ = 146°, ψ = 102°) for β-Cellotriose undecaacetate between the non-reducing and middle residues, X4 (ϕ = 135°, ψ = 98°) for CTA II polymer, and X5 (ϕ = 144°, ψ = 72°) for CTA I polymer, respectively.

ready discussed in the analysis of the CTA monomer conformation, three staggered conformations at χ61 take almost the same energies. This agrees with the above results that the dihedrals of χ61 take various conformations according to the environment surrounding the residues. Stipanovic and Sarko[9] as well as Roche et al.[13] measured the X-ray diffraction of CTA I and CTA II crystals respectively, and they estimated that the dihedral of χ61 takes the *gg* conformation in both samples. However, Leung et al.[28] obtained that χ61 of per acetylated cellobiose takes both *gg* and *gt* conformations. Moreover, Perez and Brisse[29] also indicated that χ61 of a reduced residue for per acetylated cellotriose takes the *gt* conformation, although χ61 of other residues take *gg*. In addition, Rao et al.[31] showed that χ61 takes the *gt* type to the same extent as *gg* by measuring the ^{1}H NMR of CTA in a solvent and an MM calculation of a CTA monomer. These lines of evidence also support our calculations that the staggered conformations of χ61 have almost the same energies, and that it easily changes the conformation according to the environments.

On the other hand, most of the dihedral angles of the acetyl residues at the 2 and 3 positions take the *cis* conformation, as shown in Table 3. That is, χ21, χ22, χ31, and χ32 were all close to 0°. Those conformations can essentially be considered to prefer the *cis* position, while the acetyl residue at the 6 position can rather freely rotate.

Molecular Dynamics of CTA Hexamer. In order to investigate the solvent structuring of DMSO around the CTA polymer, a molecular dynamics simulation was performed using a CTA hexamer as a model molecule. As the starting structure of the simulation, the glycosidic dihedral angles of the CTA hexamer were all set at the value of the "A" well, which is the lowest energy structure for the CTA dimer. However, two acetyl residues of the dimer at the 6 positions had different orientations of *gt* and *tg* in the A well. As discussed concerning the monomer conformation, there is almost no energy difference among three staggered conformations of the acetyl residue at the 6 position. This is still the same as in the case of the oligomer CTA. Actually, the potential energies were found to be almost the same when we compared the CTA hexamer with two types of acetyl residue orientations at the 6 position; one has *gt* in all residues, and the other has a repetition of *gt* and *tg*. Therefore, the acetyl side-chain conformations were all set to the energy minimum structure of the CTA monomer optimized by an ab initio calculation as our starting structure; that is, the conformations of acetyl residues at the 6 position were all set at *gt*. The resulting initial structure of the CTA hexamer is shown in Fig. 4. In order to clarify the figure, the position of CM2 in each CTA residue is indicated. The top view of the CTA well indicates that it is a helix with a rotation of 60° per monomer turn. A molecular dynamics simulation was performed for 1 ns on this hexamer with the surrounding 2020 DMSO molecules.

The trajectories of the glycosidic dihedral angles of (ϕ, ψ)

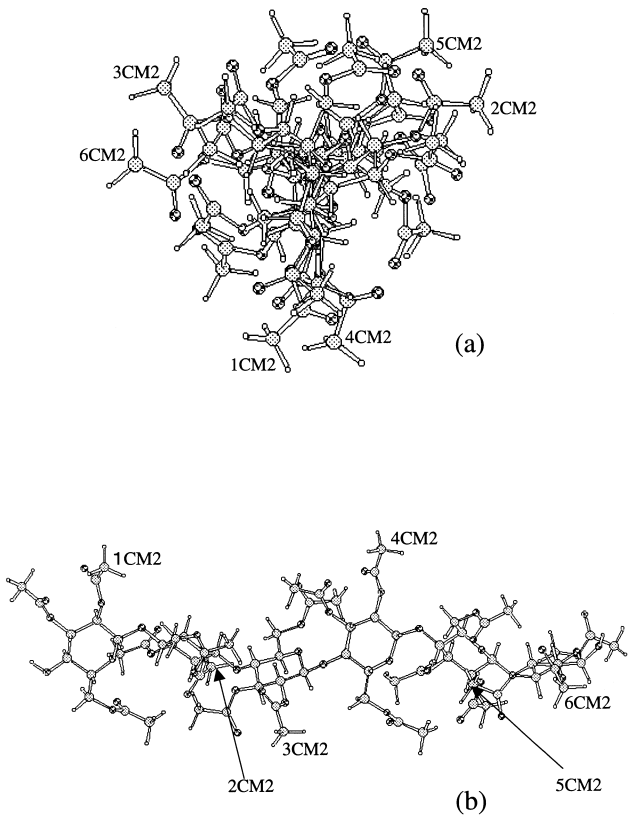

Fig. 4. Top (a) and side view (b) of the initial structure of the hexamer CTA. The dihedral angles of ϕ and ψ are all set at the global minimum value at A well. The acetyl methyl carbon at 2 position for each residue is shown.

were analyzed and the results were superimposed upon the adiabatic potential-energy map, as shown in Fig. 5. Although there is an exception (e) as an end effect and short excursion toward the C well in (c), all other trajectories were found to remain at their original position of A. In order to evaluate the extent of the fluctuation on ϕ and ψ, the dihedral angles of ϕ and ψ are plotted against time in Fig. 6. In this figure, only the time courses of ϕ and ψ between the residues of CTA2 and CTA3 are plotted as an example. It can be seen that the glycosidic dihedrals are swinging around the average values with a range of 30°. The fluctuation of ϕ may be slightly larger than ψ. This tendency is almost the same regarding all other glycosidic dihedral angles. The above results indicate that CTA exists in DMSO as a stable conformation during the time investigated. Therefore, all of the time lengths of the trajectories can be used to analyze of the solvent structure around the CTA molecule in the following section. Before discussing the solvent analysis, we examine the whole structure of this oligosaccharide in slightly more detail. For this purpose, it is convenient to use the virtual angle θ,[8] rather than ϕ and ψ. This virtual dihedral angle is defined as nH1–nC1–(n + 1)C4–(n + 1)H4. In this definition, the carbon atoms of nC1 and (n + 1)C4 are linked virtually with each other. By using this definition, the relative orientation between the adjacent pyranose rings can be evaluated. For example, when the virtual angle θ is 0°, the conformation becomes a 2/1 helix. Figure 7 shows the time courses of the virtual angle θ for all glycosidic linkages. Figure 7(e) again shows that the end residue effect and the virtual angle are shifted from 60° to 120°. However, all other virtual angles keep their average value at around 60°. This indicates that the structure is twisted by 60 degrees at every adjacent glucose ring, that is, CTA keeps a 3/2 helix in our simulation.

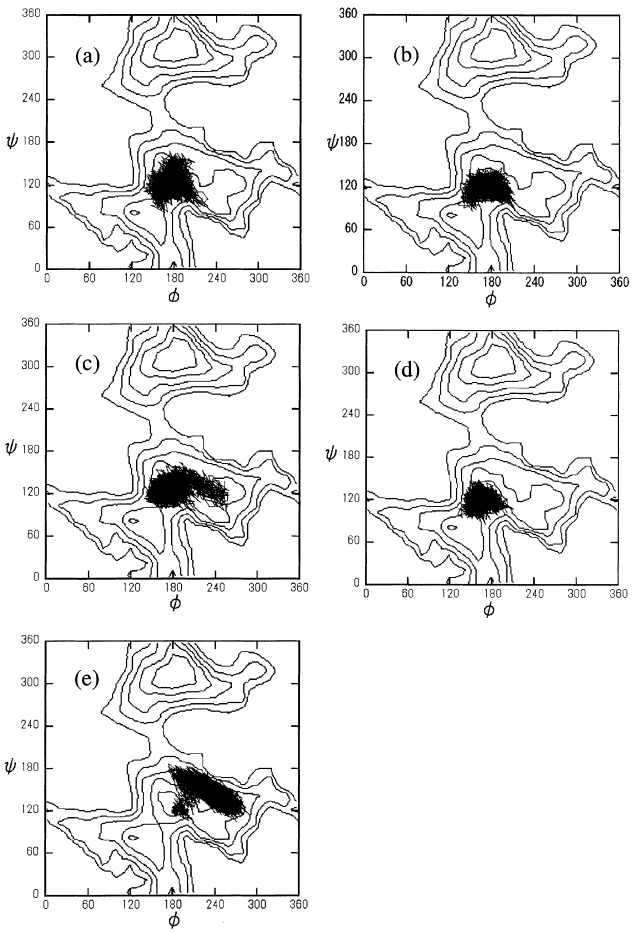

Fig. 5. Trajectories of the ϕ and ψ glycosidic dihedral angles of the hexamer CTA in DMSO started from the global minimum well of A, which were superimposed on the adiabatic energy map. The (ϕ, ψ) trajectories are between the linkages of CTA1 and CTA2; (a), CTA2 and CTA3; (b), CTA3 and CTA4; (c), CTA4 and CTA5; (d), CTA5 and CTA6; (e), respectively.

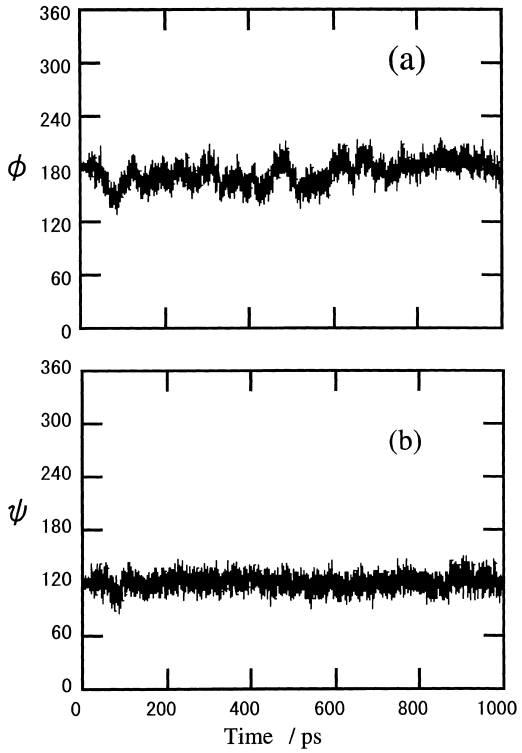

Fig. 6. Time histories for the glycosidic dihedral angles of ϕ; (a) and ψ; (b) between CTA2 and CTA3 residues of the hexamer CTA in DMSO.

Based on the NOESY NMR experiment of CTA in DMSO, Tezuka[1] showed that there are strong cross peaks of through-space interactions between the acetyl methyl protons at the 3, 6 and 2,6 positions, respectively. Based on their results, we examined the distances of these protons from our stored coordinate sets. Since there are three hydrogen atoms on an acetyl methyl residue, the NMR signal should be the average from these protons. Thus, in our analysis, the distances between the acetyl methyl carbons were analyzed instead of taking an average of these protons. Some of the results of the distance between the acetyl methyl carbons at the 2 and 6 positions and between the 3 and 6 positions are shown in Fig. 8. Because the distances between these carbons in the same glucose residue are large and do not satisfy the NMR results, typical cases of the inter-residue distances between CTA2 and CTA3 and between CTA4 and CTA5 are shown in the figure. To avoid the

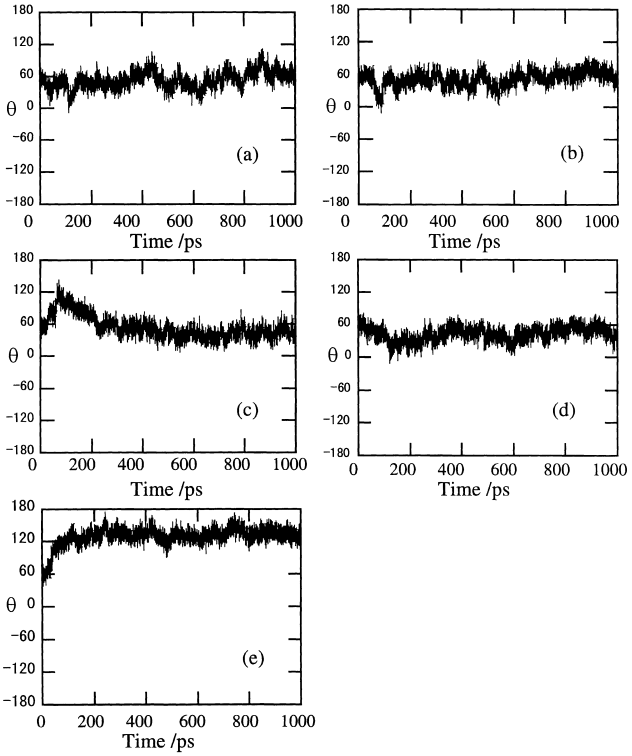

Fig. 7. Time histories for the virtual angle θ between the linkages of CTA1 and CTA2; (a), CTA2 and CTA3; (b), CTA3 and CTA4; (c), CTA4 and CTA5; (d), CTA5 and CTA6; (e) residues of hexamer CTA in DMSO.

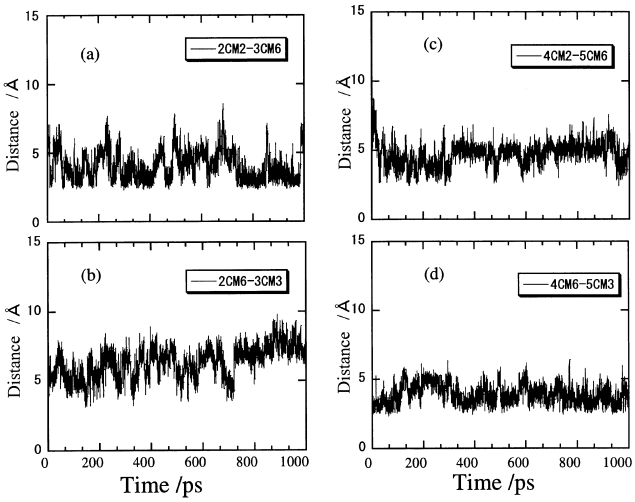

Fig. 8. Time histories of the distance between acetyl methyl carbons of hexamer CTA in DMSO. The distances are between 2CM2 and 3CM6; (a), 2CM6 and 3CM3; (b), 4CM2 and 5CM6; (c), and 4CM6 and 5CM3; (d), respectively.

end effect, the end residues were not included in the analysis. It can be seen that most of the distances existed at around 5 Å in all time courses. When the distance between the methyl carbons was shorter than 5 Å, the distance between their acetyl methyl protons should also be less than that. This is in accord with the results of the NOESY signals. It indicates that the acetyl residue conformation was also well-reproduced in our simulation. It should be mentioned that the time scale of the simulation was apparently shorter than that of NOESY experiment. This is important when a molecule takes various kinds of conformations. In this case, the simulation results should be averaged over all conformations to mimic the long time averages of the NMR. However, in our simulation, the molecule remained in only one conformation. Therefore, we did not consider the difference in the time scale in this study.

Analysis of the Solvation. Solvation is considered to have a great influence on the main chain and the side-chain conformations of CTA in DMSO. In order to investigate the solvation concerning how the DMSO molecules are spatially oriented around CTA, the radial distribution functions (RDF) of DMSO molecules were analyzed around some selected atom sites of CTA. After considering various types of combination of atoms, one was selected from atoms in CTA for the center of the RDF analysis, and the other was an atom in DMSO; the largest first peak of the radial distribution function was obtained between the oxygen atoms of DMSO (ODM) and the acetyl methyl carbon atoms of CTA. The results are shown in Fig. 9 (a). In the figure, the data of RDF obtained from all sites of acetyl methyl carbons in CTA2 to CTA5 (to avoid the end effect, the end residues were not included in these RDF analysis.) were simply superimposed. This is because the RDF first peak heights of the acetyl methyl carbons did not strongly depend on the difference in the position of acetylation. Actually, although the average peak height in Fig. 9 (a) was 2.68 at the 2 and 3 positions, and 3.18 at the 6 positions, their values at every site are scattered from 2.30 to 3.58. Therefore, the difference in the position of acetylation was not considered in this

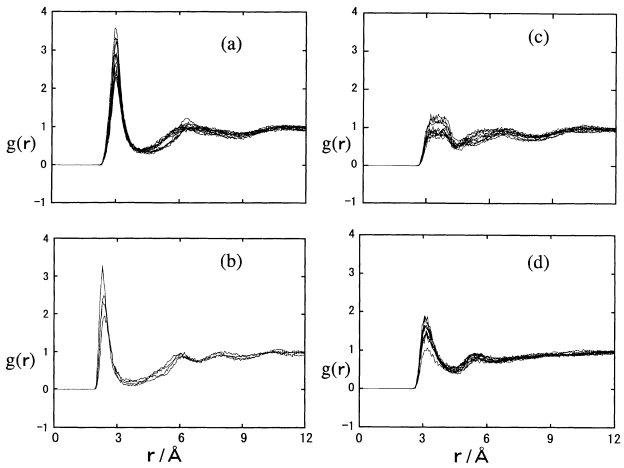

Fig. 9. Pair distribution functions for oxygen atoms of DMSO as a function of the distance from acetyl methyl carbons; (a), ring protons H1; (b), acetyl carbonyl carbons; (c) of hexamer CTA. The results of the pair distribution function for methyl residues of DMSO as a function of the distance from acetyl carbonyl oxygens of hexamer CTA are shown in (d). The lines indicated the results calculated from all sites from CTA2 to CTA5 which are simply superimposed without any distinction of the acetyl position and the residues. (The end residues were not included to avoid end effect.)

analysis. From the present results, it appears that the DMSO molecule most strongly solvated to the acetyl methyl carbons of CTA in order to face the DMSO oxygen towards them. Because the signs of both partial atom charges of the acetyl methyl carbon and the oxygen atom of DMSO are minus, these atoms should attract each other through the positively charged acetyl methyl hydrogen atom. Apparently, this suggests the existence of a C–H···O type interaction. A similar interaction was also found in the RDF between the CH proton at the 1 position of a glucose ring and the DMSO oxygen, as shown in Fig. 9 (b). Vaisman and Berkowitz[32] performed a molecular dynamics simulation on a DMSO–water binary system, and suggested that the C–H···O type hydrogen-bond interaction exists between the methyl hydrogen and the oxygen atom in different DMSO molecules. Recently, a growing amount of evidence, coming mostly from neutron-diffraction data on small molecules, show that C–H···O has a significant influence on structural chemistry.[33] The C–H···O type hydrogen bonds have also been suggested to participate in the stabilization of biopolymers, like nucleotides.[34] Auffinger et al.[35] performed molecular dynamics simulations of the anticodon hairpin of $tRNA^{Asp}$, and showed structuring effects of the C–H···O hydrogen bonds. In addition, Taylor and Kennard[36] showed that the C–H···O bonds occur for C···O distances of between 3.0 Å and 4.0 Å. These lines of evidence suggest that similar C–H···O type hydrogen bonding would occur between the acetyl methyl residues or the ring CH of CTA and the DMSO oxygen.

Other characteristic interactions found in the analysis of the radial distribution function are as follows. Figure 9 (c) shows the radial distribution function of the DMSO oxygen (ODM) around the acetyl carbonyl carbon atoms of CTA. Similarly, Fig. 9 (d) shows the radial distribution function of methyl residues of DMSO (united atom CD1) around the acetyl carbonyl oxygen of CTA. However, these signals were weak compared to the interactions mentioned above. The dependence of these interactions on the position of acetylation was again not seen in these cases. Although the dipole-dipole interaction between carbonyl groups of CTA and DMSO S–O groups is generally expected to be the largest, the result of our simulation indicated that it is not. We think that this is because of a steric hindrance around the carbonyl group of CTA. DMSO molecules may more easily approach outer methyl residues than the inner carbonyl groups. The values of the peak intensity and the distance at the first peak of each RDF were averaged, and are summarized in Table 4 along with the values of the coordination number of atoms calculated within the first peak. Kamide et al.[37] measured the chemical shift of the acetyl methyl proton and carbonyl carbon atoms of CTA (DS = 2.92) in various solvents using pulse-Fourier ^{1}H and ^{13}C NMR. From these chemical shifts, they speculated that the DMSO oxygen would coordinate to the acetyl methyl proton and the acetyl carbonyl carbon of CTA. They also did not observe the difference in the coordination based on the positions of the acetyl residues. These results were similar to those found in our simulation.

The radial distribution function is a convenient tool to know how DMSO is oriented around the CTA molecules. However, it is insufficient to know the dynamic behavior of individual DMSO molecules, namely to know how, when, and which DMSO molecule coordinates to CTA, since the radial distribution function gives only their average values. Subsequently, we analyzed the behavior of each individual DMSO molecule, which closely approaches to CTA, in detail. Typical cases are shown in Fig. 10. This figure shows the time histories of DMSO atoms when they closely approach to one of two, or both, selected acetyl residues. A typical example of this analysis is shown in this figure. Here, two selected acetyl residues are at the 6 position of CTA4 and its adjacent residue at the position of CTA5. The analysis was performed on the last 500 ps time steps of the simulation where the conformation reached a steady state, as shown in Fig. 7. In the figure, the red lines show the time steps of DMSO oxygen atoms (ODM) when they approached less than 4 Å from the acetyl methyl carbon atom of CTA4 at the 6 position (4CM6). A distance of 4 Å was taken from the average value of the RDF first minimum. Similarly, the blue lines show the time steps of the same oxygen atoms (ODM) which approached less than 4 Å from the acetyl methyl carbon atom of CTA5 at the 3 position (5CM3). The vertical axis indicates the sequential number of 8080 atoms, which consists of 2020 DMSO molecules in our simulation. Therefore, the horizontal lines will overlap on the figure when the same DMSO oxygen atom (ODM) approaches simultaneously to two acetyl methyl carbons of 4CM6 and 5CM3. Actually, we can see typical examples of the overlapping of the lines in Fig. 10, such as, the DMSO oxygen atoms of No. 7445 and No. 6561 and so on. Moreover, once they are trapped by acetyl methyl residues, they tend to keep approaching for a while. This result indicates the possibility that the oxygen atom of a DMSO molecule interacts not only with one acetyl

Table 4. Averaged Characteristic Feature of the First Solvation Shell Obtained by Radial Distribution Function between the Selected CTA Atom Sites and DMSO Atoms

Type of atom pair	Average distance of first peak, r	Average value of first peak, g(r)	Average number of atoms within the first peak, n
Atoms of CTA Site–Atoms of Solvent	Å		
Acetyl methyl C–ODM	3.0	2.8	2.1
Ring proton H1–ODM	2.3	2.5	1.2
Acetyl carbonyl C–ODM	3.5	1.1	1.9
Acetyl carbonyl O–CD1	3.1	1.6	1.9

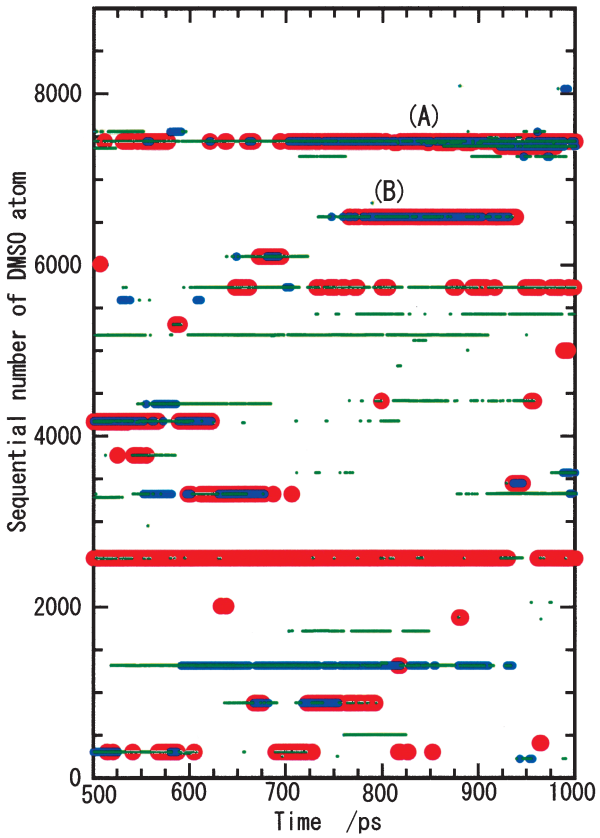

Fig. 10. DMSO atoms within 4 Å from selected atom sites on hexamer CTA were shown. The ordinate is the sequential serial number of DMSO atoms defined in this work. The red lines indicate the time when the DMSO oxygen atoms (ODM) exist within 4 Å from 4CM6. Similarly, the blue lines indicate the time of the ODM exists within 4 Å from 5CM3. The green lines indicate one of the methyl residues (CD1, CD2) in DMSO exist within 4 Å from carbonyl oxygen either at 4O61 or 5O31.

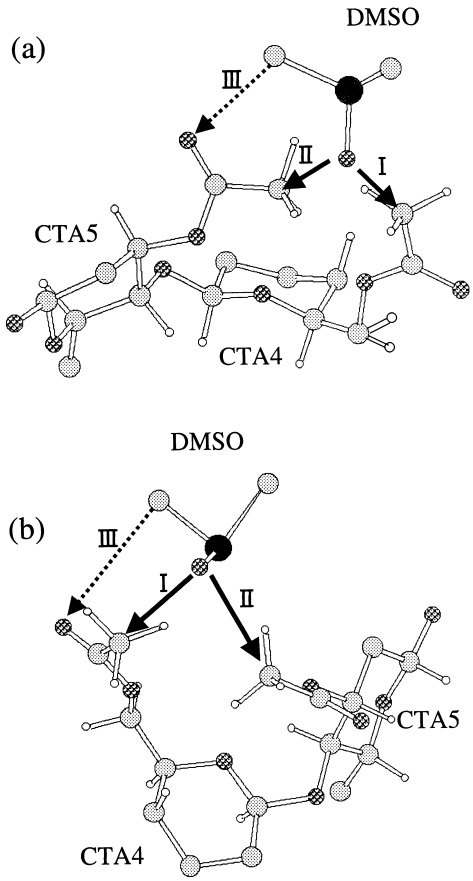

Fig. 11. Two snapshot figures at 840 ps in (A) region; (a), and at 800 ps in (B) region; (b), were shown. The regions (A) and (B) are shown in Fig. 10. In the figure, only the residues of CTA4 and CTA5 are depicted, and most of the acetyl side chains were omitted except the interaction parts, for simplification.

methyl residue, but also with two neighboring acetyl methyl residues simultaneously. These DMSO molecules may be considered to form a bridge between two acetyl residues.

On the other hand, the thin green lines in the figure indicate that one of the united atoms of methyl residues (CD1, CD2) in DMSO exists within less than 4 Å from the carbonyl oxygen atoms either at the 6 position of CTA4 (4OAc6) or the 3 position of CTA5 (5OAc3). Because the number was added sequentially, the atoms belonging to the same DMSO molecule show their lines at almost the same positions on the vertical axis in Fig. 10 (for example, the atoms in a certain DMSO molecule were numbered as SDM = 2000, ODM = 2001, CD 1 = 2002, and CD 2 = 2003). Especially, at the points indicated as (A) and (B) in the figure, it can be observed that the three different lines overlap each other. Therefore, in this region, it can be considered that a DMSO molecule interacts with CTA, not only through the formation of a bridge with two acetyl residues via a DMSO oxygen, but also through an interaction between the methyl residues of DMSO (CD1,CD2) and the carbonyl oxygen of the acetyl residue.

A snapshot of the solvated structure between DMSO and CTA at a time of 840 ps in (A) is shown in Fig. 11 (a). It can be seen that the oxygen atom of DMSO approaches two acetyl methyl residues at the 6 position of CTA4 and the 3 position of CTA5 simultaneously and, at the same time, a methyl residue of DMSO (CD1 or CD2) approaches to carbonyl oxygen atom at 3 position of CTA5 (5OAc3). Similarly, a snapshot at a time of 800 ps in (B) is shown in Fig. 11 (b). It can also be seen that the oxygen atom of DMSO interacts with acetyl methyl residues at the 6 position of CTA4 and the 3 position of CTA5 simultaneously. However, the methyl residue of DMSO interacts with the acetyl carbonyl oxygen not at the 3 position of CTA5 (5OAc3), but to another one at the 6 position of CTA4 (4OAc6) instead. These interactions are indicated in the figure as types I, II and III, respectively, for the convenience of the following discussion.

As a result of examining various possibilities concerning the formation of different kinds of bridges, the coordination types shown in Fig. 11 were confirmed to be the ones that most typically occurred in the cases of our simulation. Thus, further investigations were made on types I, II, and III, quantitatively. Table 5 shows the total time of formation for each type of bridge and its average number in each time step during the last 500 ps simulation. It can be seen that types I and II formed 2.5

Table 5. Types of the Interaction Which Was Formed between Acetyl Residues of CTA and DMSO Solvent Which Were Analyzed between 4CM6 and 5CM3

Case	Type	Total time of the formation in last 500 ps trajectory	Number of formation per each time step	c, d/a
		ps		%
a	I	1249	2.5	—
b	II	869	1.7	—
c	I + II	448	0.9	c/a = 36
d	I + II + III	176	0.4	d/a = 14

and 1.7 times per each time step on the average, respectively. These cases where types I and II occurred simultaneously were also examined, and are summarized in the same table as case (c). Such an orientation exists 0.9 times in each time step, which corresponds to 36% of the occurrence of type I. Furthermore, the conformation where all three types (I, II, and III) exist simultaneously was classified as case (d), which corresponds to the cases shown in Fig. 11. This formation exists 0.4 times in each time step, which corresponds to 14% of the occurrence of type I. The occurrence of this position would strengthen the stability of bridge formation. As a summary of these results, it became clear that two or more DMSO oxygen atoms always approach closely to acetyl methyl residues of CTA4, and 36% of those DMSO also approach to the other adjoining acetyl methyl residue simultaneously, which forms a solvation bridge through the DMSO molecule. A molecule of DMSO, which forms such an arrangement, can be considered to always exist (0.9 times) at each time step. Furthermore, an additional interaction, where the methyl residue of DMSO approaches to the acetyl carbonyl oxygen of CTA, also exists with an average of 0.4 per each time step. In the above analysis, we focused on the acetyl methyl carbon of 4CM6. However, it should be noted again that the same tendency was generally observed in other acetyl methyl carbons on different CTA residues. The interaction between DMSO and CTA through the formation of a solvation bridge would contribute to the stability of the whole conformation of CTA in the solvent.

Conclusions

In the simulation of this research, CTA kept a stable structure close to that of the 3/2 helix in DMSO solvent; also the distances between the acetyl methyl protons were in good agreement with the results obtained by the NOESY NMR experiment.[1] According to an analysis of the radial distribution function, DMSO molecules strongly solvated to CTA, especially to their acetyl methyl residues and ring protons. A further investigation on the coordination structure of the DMSO to CTA indicated that a bridged structure forms between the acetyl residues of adjacent monomers through a DMSO molecule. It would be a factor to stabilize the conformation of CTA. These lines of evidence can be considered as if CTA is tightly surrounded by DMSO molecules, and they would restrict the conformational motion of CTA and its side-chain acetyl residues.

Additionally, a neutron-diffraction analysis for pure liquid DMSO[38] indicated that the DMSO molecules have an ordered chain-like orientation with their dipole moment parallel, which is close to the crystal structure of DMSO. Moreover, adjacent DMSO molecules in neighboring chains are oriented with their dipole moment anti-parallel. Furthermore, Vaisman and Berkovitz[32] suggested the possibility of the existence of the CH···O type interaction between DMSO solvents. These interactions may form like a network structure of DMSO solvents around the whole CTA molecule. The above consideration also supports the picture of our speculation that CTA is tightly surrounded by DMSO molecules, which would restrict the conformational motion of CTA. We want to conduct a further analysis on these network structures around the CTA molecule.

This work suggests that the DMSO solvent would play an important role in the conformational stability of CTA in solution. These specific interactions between the CTA and the solvent should of course depend on the nature of the solvent. Especially, the properties of CTA in chroloform is important to investigate, as was suggested by Buchanan et al,[8] and Tezuka.[1] The modeling work of CTA concerning this solvent will be discussed in the near future. A detailed investigation of the relation between the nature of the various solvents and the conformation would provide important information on the control of the solution properties.

The authors thank Daicel Chemical Co., Ltd. for financial support.

References

1 Y. Tezuka, *Biopolymers*, **34**, 1477 (1994).

2 H. M. Spurlin, in "Cellulose And Cellulose Derivatives," ed by E. Ott, H. M. Spurlin, and H. W. Graffin, Interscience publishers, New York (1955).

3 V. Stannett, "Cellulose Acetate Plastics," Temple press, London (1950).

4 K. Singh and A. K. Tiwari, *J. Colloid Interface Sci.*, **210**, 241 (1998).

5 H. J. M. Hijnen and J. A. M. Smit, *J. Colloid Interface Sci.*, **218**, 243 (1999).

6 T. Murata and A. Tanioka, *J. Colloid Interface Sci.*, **209**, 362 (1999).

7 Y. Tsunashima and K. Hattori, *J. Colloid Interface Sci.*, **228**, 279 (2000).

8 C. M. Buchanan, J. A. Hyatt, and D. W. Lowman, *J. Am. Chem. Soc.*, **111**, 7312 (1989).

9 A. J. Stipanovic and A. Sarko, *Polymer*, **19**, 3 (1978).

10 H. Kono, Y. Numata, N. Nagai, T. Erata, and M. Takai, *Carbohydr. Res.*, **322**, 256 (1999).

11 H. Kono, Y. Numata, N. Nagai, T. Erata, and M. Takai, *J.*

Polym. Sci., Part A, **37**, 4100 (1999).
12 P. Zugenmaier, *J. Appl. Polym. Sci., Appl. Polym. Symp.*, **37**, 223 (1983).
13 E. Roche, H. Chanzy, M. Boudeulle, R. H. Marchessault, and P. Sundararajan, *Macromolecules*, **11**, 86 (1978).
14 C. L. Brooks, Ⅲ, M. Karplus, and B. M. Pettitt, in "Proteins: A Theoretical Perspective of Dynamics, Structure, and Thermodynamics," John Wiley & Sons, New York (1988).
15 B. R. Brooks, R. E. Bruccoleri, B. D. Olafson, D. J. States, S. Swaminathan, and M. Karplus, *J. Comput. Chem.*, **4**, 187 (1983).
16 S. N. Ha, A. Giammona, M. Field, and J. W. Brady, *Carbohydr. Res.*, **180**, 207 (1988).
17 M. J. Frisch, G. W. Trucks, H. B. Schlegel, P. M. W. Gill, B. G. Johnson, M. A. Robb, J. R. Cheeseman, T. A. Keith, G. A. Petersson, J. A. Montgomery, K. Raghavachari, M. A. Al-Lahan, V. G. Zakrzewski, J. V. Ortiz, J. B. Foresman, J. Cioslowski, B. B. Stefanov, A. Nanayakkara, M. Challacombe, C. Y. Peng, P. Y. Ayala, W. Chen, M. W. Wong, J. L. Andres, E. S. Replogle, R. Gomperts, R. L. Martin, D. J. Fox, J. S. Binkley, D. J. Defrees, J. Baker, J. P. Stewart, M. Head-Gordon, C. Gonzalez, and J. A. Pople, "Gaussian 94, version D.4," Gaussian Inc., Pittsburgh PA (1995).
18 J. J. P. Stewart, *J. Comput. Chem.*, **10**, 209 (1989).
19 B. H. Besler, K. M. Jr. Merz, and P. A. Kollman, *J. Comput. Chem.*, **11**, 431 (1990).
20 U. C. Singth and P. A. Kollman, *J. Comput. Chem.*, **5**, 129 (1984).
21 M. S. Skaf, *J. Chem. Phys*., **107**, 7996 (1997)
22 H. Liu, F. Muller-plathe, and W. F. van Gunsteren, *J. Am. Chem. Soc.*, **117**, 4363 (1995).
23 K. Ueda and J. W. Brady, *Biopolymers*, **38**, 461 (1996).
24 K. Ueda, M. Saiki, and J. W. Brady, *J. Phys. Chem. B*, **105**, 8629 (2001).
25 K. Ueda, K. Iwama, and H. Nakayama, *Bull. Chem. Soc. Jpn.*, **74**, 2269 (2001).
26 M. K. Dowd, P. J. Reilly, and A. D. French, *J. Comput. Chem.*, **13**, 102 (1992).
27 P. Ewald, *Ann. Phys.*, **64**, 253 (1921).
28 F. Leung, H. D. Chanzy, S. Perez, and R. H. Marchessault, *Can. J. Chem.*, **54**, 1365 (1976).
29 S. Perez and F. Brisse, *Acta Cryst.*, **B33**, 2578 (1977).
30 B. J. Hardy and A. Sarko, *J. Comput. Chem.*, **14**, 831 (1993).
31 V. S. Rao, F. Sauriol, A. S. Perlin, and M. T. P. Viet, *Can. J. Chem.*, **63**, 2507 (1985).
32 I. I. Vaisman and M. L. Berkowitz, *J. Am. Chem. Soc.*, **114**, 7889 (1992).
33 T. Steiner and W. Saenger, *J. Am. Chem. Soc.*, **114**, 10146 (1992).
34 S. T. Rao and M. Sundaralingam, *J. Am. Chem. Soc.*, **92**, 4963 (1970).
35 P. Auffinger, S. Louise-May, and E. Westhof, *J. Am. Chem. Soc.*, **118**, 1181 (1996).
36 R. Taylor and O. Kennard, *J. Am. Chem. Soc.*, **104**, 5063 (1982).
37 K. Kamide, M. Saito, K. Kowsaka, and K. Okajima, *Polymer J.*, **19**, 1377 (1987).
38 H. Bertagnolli and E. Schultz, *Ber. Bunsenges. Phys. Chem.*, **93**, 88 (1989).